UNIVERSITAT POLITÈCNICA
DE CATALUNYA
BARCELONATECH

UPCommons

Portal del coneixement obert de la UPC

http://upcommons.upc.edu/e-prints

Heidary Yazdi, Seyed Saeid; Rouzbehi, Kumars; Candela, José Ignacio; Milimonfared, Jafar; Rodríguez, Pedro (2017) Analysis on impacts of the shunt conductances in multi-terminal HVDC grids optimal power-flow. *IECON 2017 - 43rd IEEE Annual Conference of the IEEE Industrial Electronics Society, Beijing, China, Oct. 29 – Nov. 1, 2017: proceedings.* [S.l.]: IEEE, 2017. Pp. 121-125 Doi: 10.1109/IECON.2017.8216025

© 2017 IEEE. Es permet l'ús personal d'aquest material. S'ha de demanar permís a l'IEEE per a qualsevol altre ús, incloent la reimpressió/reedició amb fins publicitaris o promocionals, la creació de noves obres col·lectives per a la revenda o redistribució en servidors o llistes o la reutilització de parts d'aquest treball amb drets d'autor en altres treballs.

Analysis on Impacts of the Shunt Conductances in Multi-Terminal HVDC Grids Optimal Power-Flow

Seyed Saeid Heidary Yazdi*, Kumars Rouzbehi***, J. Ignacio Candela**
Jafar Milimonfared*, and Pedro Rodriguez**,***
* Amirkabir University of Technology, Tehran, Iran
** Technical University of Catalonia, Barcelona, Spain
***Loyola University Andalucia, Seville, Spain
saedheidary@aut.ac.ir

***Abstract*—This study deals with impacts of the shunt conductances associated with HVDC cables and VSC-HVDC stations on optimal operation of Multi-Terminal HVDC (MT-HVDC). In this study, for the first time, shunt conductances are integrated to HVDC Optimal Power- Flow (OPF) program that is executed at the Power Dispatch Center (PDC) of the MT-HVDC grid. With the objective of losses minimization, optimal reference operation points of the VSC-HVDC stations are derived. The operating points of the power converter stations are adjusted based on the calculations performed in the dispatch center. CIGRE DCS3 MT-HVDC grid, structured by CIGRE B4 working group, is taken as the test platform. Test results have revealed the optimum voltages and loss pattern change. Moreover, the findings are compared with the case of neglecting the shunt conductances.**

Index Terms*—*CIGRE DCS3 HVDC grid, dc Optimal power flow, multi-terminal HVDC grid.

I. INTRODUCTION

The evolution of Multi-Terminal HVDC (MT-HVDC) grids is mainly because of two main drivers: firstly, their sufficiency to link multiple ac networks that are operating at distinct ac voltage levels even at different frequencies [1], secondly they are suitable for integrating of large-scale offshore wind energy to main ac grids [2, 3]. In recent years, extensive industrial and academic studies on MT-HVDC grids have been conducted [4, 5]. Since 1951, there has been evidence of up to 180 predominant two-terminal point-to-point HVDC projects which have been implemented worldwide [6]. During the last decade, some HVDC systems have been extended with additional power converter stations to form the first operational MTDC systems. By means of the progress and getting the popularity of high-power Voltage Source Converter (VSC)s, the prospect of the MT-HVDC networks, comprised of several VSC-HVDC stations has converted to a real opportunity.

In the framework of this emerging paradigm, MT-HVDC grid optimal operation is of high importance since it is directly translated to higher delivered power and hence higher revenue. In the context of MT-HVDC grid two-layered control, DC power flow, DC Optimal Power Flow (DC OPF) and energy market-related strategies are usually addressed at the secondary control layer. Whereas, control of power converters, direct voltages, and power sharing are assigned to the primary control layer. Indeed, appropriate reference settings are sent to the VSC-HVDC stations in a prescribed time intervals by the power dispatch control center of the MT-HVDC grid [7, 8].

Several numbers of research have focused on the designing of the secondary control layer to minimize transmission losses [9-12], and total transmission and converters losses [13] considering voltage-droop control [14]. It is done by calculating optimum droop reference voltages. Also, a droop control gain design methodology is proposed in [15] for optimal power sharing among the VSC-HVDC stations in order to maximize the power transmission capacity. Also, [16] considered adaptive droop control gains according to cable resistances to minimize the losses and prevent converter overvoltage. Moreover, [17, 18] proposed generazlized droop control framework and unified reference controller for onshore side converters to control direct voltages and share the burden of dynamic frequency response among HVDC converters respectively.

To the best of the authors knowledge, none of these studies is investigated impacts of the shunt conductances associated with HVDC cables and VSC-HVDC stations on the optimal operation of the MT-HVDC grid. Indeed, they are simply neglected in their modelings. However, these shunt conductances lead to a significant change in DC OPF results that is the focus of this research.

This paper contributes to the state of the art by deriving a static model of MT-HVDC grid taking conductances of HVDC cables and VSC-HVDC stations into account to assess their impacts on DC OPF result pattern. The optimization results which are calculated at the secondary control layer are passed to voltage droop based primary control layer. CIGRE DCS3 MT-HVDC grid is selected as our test platform in order to validate the claims of this study.

This paper is organized as follows: Formulation of DC OPF and its solving approach are presented in sections II and III, respectively. Sections IV and V draw the test results and main conclusions respectively.

II. FORMULATION OF DC OPF PROBLEM

The definition of DC OPF problem can be inspired by the well-known OPF problem of AC power system [19] with some modifications. In fact, the DC OPF can be considered as a simplified type of the AC grids OPF, since the reactive power does not longer exist in MT-HVDC grids.

Optimal operation of MT-HVDC grids can be assessed by means of several technical, economical and/or other criterions. However, the present study focuses on minimization of the MT-HVDC grid total losses ($f(\mathbf{V})$) by means of solving the DC OPF problem. The DC OPF problem is formulated by (1)–(5)

assuming n grid side VSC-HVDC stations, p intermediary buses (without generation and loads), and m wind farms as:

$$f(\mathbf{V}) = \mathbf{V}^T \mathbf{Y} \mathbf{V} \tag{1}$$

$$\mathbf{V}^T \mathbf{Y}_P \mathbf{V} = \sum_{i=1}^{n+p+m} \left(g_{ii} V_i^2 \right) \tag{2}$$

$$\mathbf{V}^T \mathbf{Y}_S \mathbf{V} = \sum_{i=1}^{n+p+m} \sum_{j=(i+1)}^{n+p+m} g_{ij} \left(V_i - V_j \right)^2 \tag{3}$$

where $\mathbf{V}=[V_1, V_2, \ldots, V_{m+n+p}]^{\mathrm{T}}$ and $\mathbf{Y}$ denote the MT-HVDC vector of buses voltage and admittance matrix respectively. Moreover, g_{ii} and g_{ij} respectively indicate the sum of conductances appeared between bus i and ground and the net conductance seen betwixt buses i and j. HVDC overhead lines and cables are modeled by a lumped π model [20]. $\mathbf{Y}$ is divided into the elements influenced by the shunt conductances ($\mathbf{Y_P}$) and the remaining parts ($\mathbf{Y_S}$). Hereafter, losses defined by (2) and (3) will be called "shunt losses" and "series losses", respectively. They are quadratically dependent on bus voltages and HVDC lines currents respectively. Therefore, they change in opposite directions with respect to MT-HVDC grid bus voltage levels. For instance, as direct voltage levels increase to reduce the currents level (and therefore series losses), the shunt losses increase. Hence, there should be a trade-off determined by the DC OPF routine. Several equality and inequality constraints are applied to the objective function:

$$\mathbf{g}(\mathbf{V},\mathbf{P}) = 0 \tag{4}$$

$$|P_i| < P_i^{\max}, \quad i = 1,\ldots,n \tag{5}$$

$$V_{DC}^{\min} < V_{DC,i} < V_{DC}^{\max}, \quad i = 1,\ldots,(n+p+m) \tag{6}$$

$$|I_{DC,k}| < I_{DC,k}^{\max}, \quad k = 1,\ldots,L \tag{7}$$

in which L denotes the total number of HVDC overhead/cables inside the system. Here, P_i, V_{DCi}, and $I_{DC,k}$ denote the exchanged power by VSC-HVDC station i, bus i voltage and the amount of current flowing in the line k, respectively. Also, $\mathbf{P}$ represents the matrix of absorbed bus powers. The DC power flow is represented by the equality constraint ($\mathbf{g}(\mathbf{V},\mathbf{P}) = \mathrm{diag}(V_1,\ldots,V_{n+p+m})\mathbf{Y}\mathbf{V} - \mathbf{P} = 0$), and can be expanded as follows (for the case of power-voltage droop control):

$$\mathrm{diag}(V_1,\ldots,V_{n+p+m})\mathbf{Y}\mathbf{V} - \begin{bmatrix} -k_{droop,1}(V_1 - V_1^0) \\ -k_{droop,2}(V_2 - V_2^0) \\ \cdot \\ -k_{droop,n}(V_n - V_n^0) \\ 0 \\ \cdot \\ 0 \\ P_{wind,1} \\ \cdot \\ P_{wind,m} \end{bmatrix} = 0 \tag{8}$$

In which V_i^0 and $k_{droop,i}$ denotes droop reference voltage and droop slope of i th grid side VSC-HVDC station.

Constraints (3)–(5) respectively indicate the MT-HVDC grid limitations that are associated with bus voltages, VSC-HVDC stations transmitted power and the HVDC lines current. In (3), $P_i^{\max}$ stand for the utmost permissible transmitted power by the VSC-HVDC station i. In the constraint (4), $V_{DC}^{\min}$ and $V_{DC}^{\max}$ express the lower and upper admissible span for MT-HVDC grid's direct voltages, respectively. Also, the rated DC current corresponding to the k^{rd} transmission line is represented by $I_{DC,k}^{\max}$ in (5).

III. DC OPF Problem: Solving Approach

The DC OPF problem stated by (1)–(5) falls in the nonlinear constrained optimization category. Several gradient based solvers can be utilized to solve it as shown below [21]:

$$L(\mathbf{V},\mathbf{P}) = f(\mathbf{V}) + \mathbf{q}(\mathbf{V},\mathbf{P},\mathbf{I}) + \boldsymbol{\lambda}^{\mathrm{T}}.\mathbf{g}(\mathbf{V},\mathbf{P}) \tag{9}$$

In which, $\boldsymbol{\lambda}$ is the of Lagrange multipliers vector for the equality constraint presented by (2), $\mathbf{I}$ is the DC transmission lines current vector. Also, the penalty function corresponding to the inequality constraints is presented by $\mathbf{q}$:

$$\mathbf{q}(\mathbf{V},\mathbf{P},\mathbf{I}) = \sum_{i=1}^{n+p+m} \left\{ \left(V_i - V_i^{\min}\right)^2 . pf_{V^{\min},i} + \left(V_i - V_i^{\max}\right)^2 . pf_{v^{\max},i} \right\} + \sum_{i=1}^{n} \left\{ \left(P_i - P_i^{\max}\right)^2 . pf_{P^{\max},i} \right\} + \sum_{k=1}^{L} \left\{ \left(I_{DC,ki} - I_{DC,i}^{\max}\right)^2 . pf_{I,k} \right\} \tag{10}$$

where $pf_{v^{\min},i}$, $pf_{v^{\max},i}$, $pf_{P^{\max},i}$, and $pf_{I,i}$ represent penalty factors corresponding to the lower and upper limits of direct voltage, VSC-HVDC stations, and transmission lines limits, respectively. In constrained optimization problems, it is a common procedure to substitute the inequality constraint with the penalty factors, however, these factors will be zero provided that none of the constraints are violated.

DC OPF solution can be calculated in an iterative manner considering that the derivative of the Lagrangian function ($\partial L / \partial \mathbf{V}$ and $\partial L / \partial \boldsymbol{\lambda}$) should be zero at the optimum point:

$$\frac{\partial L}{\partial \mathbf{V}} = \frac{\partial \mathbf{q}}{\partial \mathbf{V}} + \frac{\partial f}{\partial \mathbf{V}} + \left[\frac{\partial \mathbf{g}}{\partial \mathbf{V}} \right]^T \boldsymbol{\lambda} \tag{11}$$

$$\frac{\partial L}{\partial \boldsymbol{\lambda}} = \mathbf{g}(\mathbf{V},\mathbf{P}) \tag{12}$$

The computed optimum droop reference voltages (V_1^0, V_2^0 and V_3^0) are applied to the primary control layer as it is shown in Fig. 1.

IV. Test Results

A) *Cigre DCS3 MT-HVDC Test Grid*

CIGRE DCS3 MT-HVDC test grid is a bipolar (±400 kV) grid and comprised of two offshore wind power plants (m=2), three grid side VSC-HVDC stations (n=3), two intermediary buses (p=2), eight HVDC cables and overhead lines (L=8). The DCS3

grid is shown in Fig. 2 and further data are reported in [20]. In this study, per unit results are given considering 500 MW and 800 kV as base power and base voltage respectively. Onshore grid side VSC-HVDC stations employ identical 60 MW/kV droop coefficients ($k_{droop,i}$) and 800 kV droop as the initial reference voltages (V_i^0). However, a set of suitable droop reference voltages will be determined later by execution of the DC OPF problem. For the sake of simplicity, the DC buses of the DCS3 are numbered as it is presented in Table I.

TABLE I.
DCS3 BUS NUMBERS

DC Bus	Bb-A1	Bb-B1	Bb-B2	Bb-B4	Bb-E1	Bb-D1	Bb-C2
Number	1	2	3	4	5	6	7

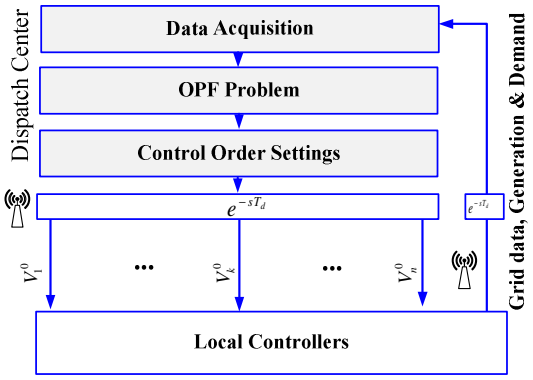

Fig.1. The hierarchal control structure of MT-HVDC grid.

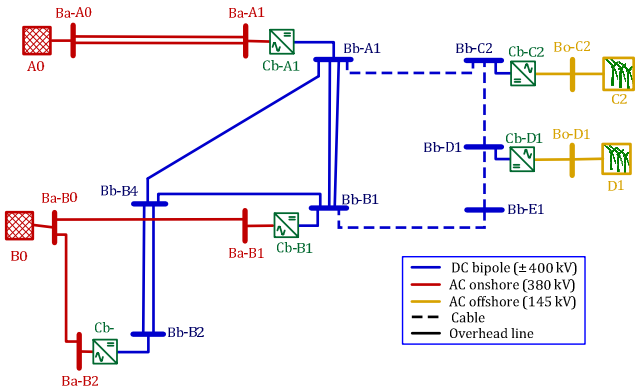

Fig. 2. Cigre DCS3 MT-HVDC test grid.

B) Impacts of DC cables and VSC-HVDCs shunt conductances on **Y** *matrix*

Parameters of DCS3 MT-HVDC grid disclose that the HVDC cables have shunt conductances of 0.048 µS/km and series resistances of 0.0095 Ω/km [20]. Moreover, 400 MVA, 800 MVA, and 1600 MVA VSC-HVDC stations exhibit 2.5 µS, 5 µS, and 7.5 µs shunt conductance respectively. Those are associated with their DC capacitors. $\mathbf{Y_P}$ and $\mathbf{Y_S}$ can be written in per-unit as:

$$\mathbf{Y}_S = \begin{bmatrix} 729.8246 & -280.701 & 0 & -112.2807 & 0 & 0 & -336.8421 \\ -280.7018 & 898.2456 & 0 & -280.7018 & -336.8421 & 0 & 0 \\ 0 & 0 & 374.2690 & -374.2690 & 0 & 0 & 0 \\ -112.2807 & -280.7018 & -374.2690 & 767.2515 & 0 & 0 & 0 \\ 0 & -336.8421 & 0 & 0 & 673.6842 & -336.84241 & 0 \\ 0 & 0 & 0 & 0 & -336.8421 & 561.4035 & -224.5614 \\ -336.8421 & 0 & 0 & 0 & 0 & -224.5614 & 561.4035 \end{bmatrix} \quad (13)$$

$$\mathbf{Y}_P = \begin{bmatrix} 0.007871 & 0 & 0 & 0 & 0 & 0 & 0 \\ 0 & 0.007871 & 0 & 0 & 0 & 0 & 0 \\ 0 & 0 & 0.004800 & 0 & 0 & 0 & 0 \\ 0 & 0 & 0 & 0 & 0 & 0 & 0 \\ 0 & 0 & 0 & 0 & 0.006144 & 0 & 0 \\ 0 & 0 & 0 & 0 & 0 & 0.010880 & 0 \\ 0 & 0 & 0 & 0 & 0 & 0 & 0.009280 \end{bmatrix} \quad (14)$$

(13) and (14) correspond to the series and shunt losses that are also defined in (1) respectively.

C) Case study ($P_{Bb\text{-}D1}$=1.9 pu, $P_{Bb\text{-}C2}$=0.9 pu)

The DC OPF results are summarized in Table II. In order to show the considerable impacts of the shunt conductances, three case studies are investigated: 1) power flow with constant 800 kV droop reference voltages 2) DC OPF problem without considering shunt conductances 3) DC OPF problem with considering shunt conductances.

Regarding the case 2, firstly the DC OPF problem is formulated without taking shunt conductances into account. Once the optimum droop reference voltages are calculated, they are passed to the power flow problem (8) which embeds the

TABLE II.
OPTİMAL POWER FLOW RESULTS

		Power Flow With Constant 1 pu Droop Reference Voltages		With Optimization, Without Considering of Shunt Conductances		With Optimization, With Considering of Shunt Conductances	
DC Bus	Control Mode	DC Voltage (pu)	Net Power (pu)	DC Voltage (pu)	Net Power (pu)	DC Voltage (pu)	Net Power (pu)
Bb-A1	Droop	1.01100	-1.05625	1.04270	-1.51592	0.96447	-1.38942
Bb-B1	Droop	1.01040	-0.99913	1.04270	-1.23060	0.96418	-1.33413
Bb-B2	Droop	1.00704	-0.67658	1.04275	0.01407	0.96417	-0.01345
Bb-B4	Intermediate	1.00885	0	1.04272	0	0.96422	0
Bb-C2	P	1.01533	0.89999	1.04703	0.90000	0.96909	0.89999
Bb-D1	P	1.01793	1.90000	1.04974	1.90000	0.97193	1.89999
Bb-E1	Intermediate	1.01416	0	1.04621	0	0.96805	0
Series Losses (pu)		0.01992		0.01632		0.01913	
Shunt Losses (pu)		0.04811		0.05123		0.04385	
Total Losses (pu)		0.06803		0.06755		0.06298	

impacts of shunt conductances.

Regarding the case first case, the shunt losses (0.04811 pu) are clearly superior to the series losses (0.01992 pu). Persistence of this superiority will be discussed in the next section regarding different wind power generations. Therefore, the DC OPF problem (the Case study 3) assigned minimum permissible droop reference voltages to the grid side VSCs ($V_1^0 = 0.95000$ pu , $V_2^0 = 0.95028$ pu, $V_3^0 = 0.96403$ pu) to decrease the shunt losses and consequently total losses. Therefore shunt losses are reduced to 0.04385 pu from 0.04811 pu that shows a % 8.85 loss reduction.

Moreover, while the currents flowing inside MT-HVDC grid are increased as a result of voltage level reduction, series losses shows surprisingly a small decrease. This is due to optimal sharing of the power among grid side VSC-HVDC stations. In this regard, the powers absorbed by Bb-A1, Bb-B1, and Bb-B2 buses are varied to 1.38942 pu, 1.33413 pu, and 0.01345 pu from 1.05625 pu, 0.99913 pu, and 0.67658 pu respectively. Finally, total losses are reduced to 0.06298 pu from 0.06803 pu which shows a %7.42 reduction.

On the other hand, the comparison of case studies 1 and 2 exhibits a different tendency in DC OPF results. Since the impacts of shunt conductances are not considered in the DC OPF problem, it assigned droop reference voltages ($V_1^0 = 1.02691$ pu, $V_2^0 = 1.02988$ pu, $V_3^0 = 1.04289$ pu) in order to maximize the MT-HVDC voltages while preserving operational constraints. In this regard, series losses are reduced to 0.01632 pu from 0.01992 pu that shows a %18.07 loss reduction. However, the voltage increase tends to increase the shunt losses from 0.04811 pu to 0.05123 pu that shows a %6.48 loss increment. Finally, total loss reduction is confined to %0.7 due to inappropriate droop reference voltages.

D) Impacts of shunt conductances in different wind power generation scenarios

The results of three case studies defined in the previous section are depicted in Fig. 3 taking different wind power generations into account. In this figure, the below and upside

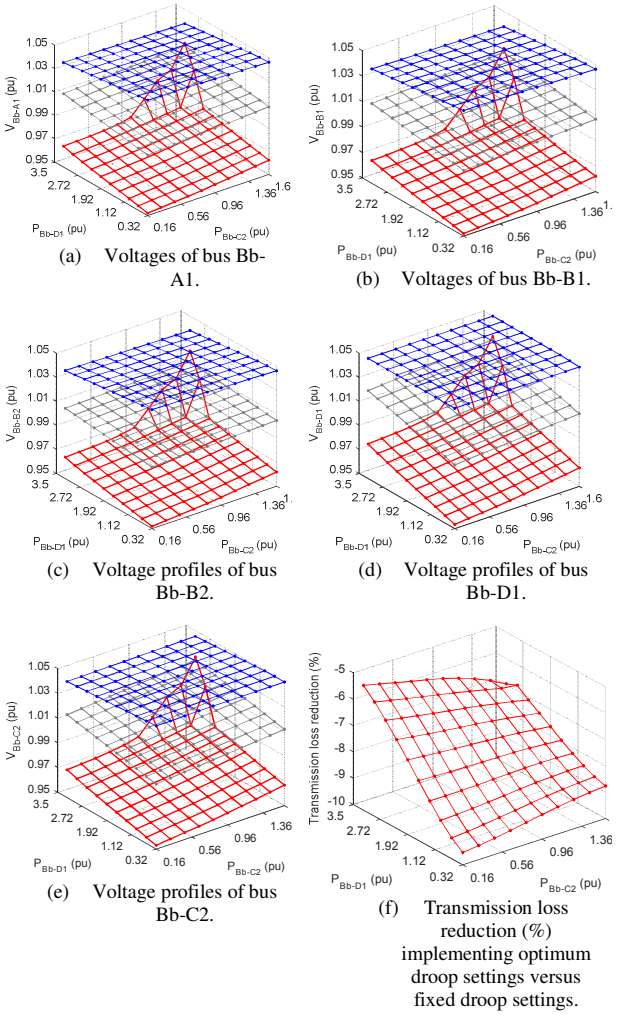

Fig. 3. The results of the case study 1 (middle planes) and the case study 2 (top planes) and the case study 3 (bottom planes)

planes stand for the case studies 3 and 2 respectively. On the other hand, the middle planes represent the case study 1.

Clearly, application of the optimum references without the effect of the shunt conductances will rise the whole MT-HVDC voltages and maximizes the offshore wind farm side voltages to reduce the series losses. Having offshore wind farm side voltages fixed at maximum permissible values (i.e., 1.05 pu), grid side voltages reduce as wind power generation increase since the voltage difference between MT-HVDC buses is required for the purpose of power flow.

On the other hand, whole MT-HVDC buses voltages are reduced to around minimum permissible values (i.e., 0.95 pu) taking the effect of shunt conductances into account. This orientation is kept unless in very high wind power generations that the series losses gain superiority in contributing to the transmission losses. Therefore, DC OPF problem tries to increase the MT-HVDC voltage levels in order to optimize transmission losses by making a tradeoff between series and shunt losses. The loss reduction is clear in Fig. 3(f), however, it is highest in low wind power generation (i.e., up to %10).

V. CONCLUSION

This study analyzed the impacts of the shunt conductances associated with HVDC cables and VSC-HVDC stations on optimal operation of the MT-HVDC grid. These conductances that can be interpreted to the shunt losses of the MT-HVDC grid are quadratically dependent on DC bus voltages. From the test platform results, it was revealed that the shunt losses are dominant in contributing to the total transmission losses except for very high wind power generations. Therefore, the DC OPF routine had a tendency to decrease MT-HVDC grid bus voltages to the proximity of the minimum permissible DC bus voltage. Conversely, this tendency has been changed to voltage increment in very high wind power generations since the MT-HVDC grid series losses become dominant. Investigating the impacts of the shunt conductances on MT-HVDC grid stability is a possible future research.

REFERENCES

[1] J. Dai, Y. Phulpin, A. Sarlette, and D. Ernst, "Coordinated primary frequency control among non-synchronous systems connected by a multi-terminal high-voltage direct current grid," *IET Generation, Transmission & Distribution,* vol. 6, pp. 99-108, 2012.

[2] X. Chen, H. Sun, J. Wen, W. J. Lee, X. Yuan, N. Li*, et al.*, "Integrating Wind Farm to the Grid Using Hybrid Multiterminal HVDC Technology," *IEEE Transactions on Industry Applications,* vol. 47, pp. 965-972, 2011.

[3] R. d. Silva, R. Teodorescu, and P. Rodriguez, "Multilink DC transmission system for supergrid future concepts and wind power integration," in *IET Conference on Renewable Power Generation (RPG 2011)*, 2011, pp. 1-6.

[4] K. Meah and A. H. M. S. Ula, "A new simplified adaptive control scheme for multi-terminal HVDC transmission systems," *International Journal of Electrical Power & Energy Systems,* vol. 32, pp. 243-253, 5// 2010.

[5] D. Van Hertem and M. Ghandhari, "Multi-terminal VSC HVDC for the European supergrid: Obstacles," *Renewable and Sustainable Energy Reviews,* vol. 14, pp. 3156-3163, 12// 2010.

[6] K. Rouzbehi, J. I. Candela, G. B. Gharehpetian, L. Harnefors, A. Luna, and P. Rodriguez, "Multiterminal DC grids: Operating analogies to AC power systems," *Renewable and Sustainable Energy Reviews,* vol. 70, pp. 886-895, 4// 2017.

[7] A. Egea-Alvarez, J. Beerten, D. Van Hertem, and O. Gomis-Bellmunt, "Hierarchical power control of multiterminal HVDC grids," *Electric Power Systems Research,* vol. 121, pp. 207-215, 4// 2015.

[8] K. Rouzbehi, J. I. Candela, A. Luna, G. B. Gharehpetian, and P. Rodriguez, "Flexible Control of Power Flow in Multiterminal DC Grids Using DC-DC Converter," *IEEE Journal of Emerging and Selected Topics in Power Electronics,* vol. 4, pp. 1135-1144, 2016.

[9] M. Aragüés-Peñalba, A. Egea-Àlvarez, O. Gomis-Bellmunt, and A. Sumper, "Optimum voltage control for loss minimization in HVDC multi-terminal transmission systems for large offshore wind farms," *Electric Power Systems Research,* vol. 89, pp. 54-63, 8// 2012.

[10] M. A. Abdelwahed and E. F. El-Saadany, "Power Sharing Control Strategy of Multi-terminal VSC-HVDC Transmission Systems Utilizing Adaptive Voltage Droop," *IEEE Transactions on Sustainable Energy,* vol. PP, pp. 1-1, 2016.

[11] K. Rouzbehi, A. Miranian, A. Luna, and P. Rodriguez, "DC Voltage Control and Power Sharing in Multiterminal DC Grids Based on Optimal DC Power Flow and Voltage-Droop Strategy," *IEEE Journal of Emerging and Selected Topics in Power Electronics,* vol. 2, pp. 1171-1180, 2014.

[12] S. S. H. Yazdi, S. H. Fathi, J. M. Monfared, and E. M. Amiri, "Optimal operation of multi terminal HVDC links connected to offshore wind farms," in *2014 11th International Conference on Electrical Engineering/Electronics, Computer, Telecommunications and Information Technology (ECTI-CON)*, 2014, pp. 1-6.

[13] M. Aragüés-Peñalba, A. Egea-Àlvarez, S. G. Arellano, and O. Gomis-Bellmunt, "Droop control for loss minimization in HVDC multi-terminal transmission systems for large offshore wind farms," *Electric Power Systems Research,* vol. 112, pp. 48-55, 7// 2014.

[14] T. K. Vrana, J. Beerten, R. Belmans, and O. B. Fosso, "A classification of DC node voltage control methods for HVDC grids," *Electric Power Systems Research,* vol. 103, pp. 137-144, 10// 2013.

[15] A. S. Abdel-Khalik, A. M. Massoud, A. A. Elserougi, and S. Ahmed, "Optimum Power Transmission-Based Droop Control Design for Multi-Terminal HVDC of Offshore Wind Farms," *IEEE Transactions on Power Systems,* vol. 28, pp. 3401-3409, 2013.

[16] J. Khazaei, Z. Miao, L. Piyasinghe, and L. Fan, "Minimizing DC system loss in multi-terminal HVDC systems through adaptive droop control," *Electric Power Systems Research,* vol. 126, pp. 78-86, 9// 2015.

[17] K. Rouzbehi, A. Miranian, J. I. Candela, A. Luna, and P. Rodriguez, "A Generalized Voltage Droop Strategy for Control of Multiterminal DC Grids," *IEEE Transactions on Industry Applications,* vol. 51, pp. 607-618, 2015.

[18] K. Rouzbehi, W. Zhang, J. I. Candela, A. Luna, and P. Rodriguez, "Unified reference controller for flexible primary control and inertia sharing in multi-terminal voltage source converter-HVDC grids," *IET Generation, Transmission & Distribution,* vol. 11, pp. 750-758, 2017.

[19] P. Preedavichit and S. C. Srivastava, "Optimal reactive power dispatch considering FACTS devices," *Electric Power Systems Research,* vol. 46, pp. 251-257, 9/1/ 1998.

[20] T. K. Vrana, Y. Yang, D. Jovcic, S. Dennetière, J. Jardini, and H. Saad, "The CIGRE B4 DC Grid Test System," 2016.

[21] S. S. Rao, *Engineering Optimization: Theory and Practice*, 4 ed.: Wiley, 2009.